ELSEVIER

Journal of Organometallic Chemistry 550 (1998) 301–308

Journal of Organometallic Chemistry

Preparation and structures of some tetraazamacrocyclic complexes of In(III) [1]

P.R. Phillips [a], M.G.H. Wallbridge [a,*], J. Barker [b]

[a] *Department of Chemistry, University of Warwick, Coventry CV4 7AL, UK*
[b] *Associated Octel, Ellesmore Port, South Wirral, L65 4HF, UK*

Received 4 March 1997

Abstract

Treatment of the dibenzo-tetraaza macrocycle, $C_{22}H_{24}N_4$ (H_2tmtaa) (**I**), with triethylindium yields the diethylindium-macrocycle complex [Et_2In(Htmtaa)] (**IV**). On heating (**IV**) is converted quantitatively into the monoethyl complex [EtIn(tmtaa)] (**V**). A single crystal X-ray diffraction study on (**V**) shows the EtIn fragment to be bonded to the four planar nitrogen atoms of the macrocycle, with a square–pyramidal geometry around the metal. Reaction of the dilithio salt of (**I**), [Li_2(tmtaa)], with $InCl_3$ yields [ClIn(tmtaa)] (**VI**), and further reaction of (**VI**) with equimolar quantities of LiR [R = C_5H_5(Cp), Me, N($SiMe_3$)$_2$, $OSiMe_3$] yields the corresponding [RIn(tmtaa)] derivatives [R = Cp (**VII**), Me (**VIII**), N($SiMe_3$)$_2$ (**IX**), $OSiMe_3$ (**X**)]. An X-ray diffraction study on (**VII**) shows an η^1-bonded Cp group, with the metal atom also bound to the four nitrogen atoms of the tmtaa ligand. © 1998 Elsevier Science S.A.

Keywords: Indium; Tetraazamacrocycle; Alkyl; Cyclopentadienyl; X-ray

1. Introduction

Organometallic derivatives of the Group 13 elements combined with macrocyclic ligands have attracted much attention [1]. Compounds of the type [RM porph)] (where M = Al, Ga, In; R = alkyl, aryl; porph = porphyrin 2-anion) are well documented, and are of interest because of the unusual co-ordination environment imposed upon the metal centre, with the metal lying above the planar N_4 unit of the prophyrin [2]. Aida and Inoue, and Takeuchi et al., have also shown that the organo–aluminium derivatives have an important application as catalysts for the polymerisation of methacrylates and other related systems [3,4].

For the Group 13 elements previous results using indium in these types of reactions are very limited [5]. Preliminary work on the reactions of the organo–indium halides $MeInX_2$ (X = Cl, I) with cyclam ([14] ane N_4) and dibenzo-18-crown-6 led to inconclusive results with the former ligand, but with the latter ionic products of the type [$InMe_2$(crown)][InX_4] or [In(Me)X(crown)][$In(Me)X_3$] were indicated from spectroscopic data [6]. Tabard et al. have reported several complexes, involving the porphyrin dianion (porph 2-), of the type [InX(porph)] (X = aryl, halide etc..) [7], and more recently a 1:1 adduct between $InMe_3$ and *N*,*N*′,*N*″-tri-*iso*-propyl-1,2,5-triaza-cyclohexane, [$Me_3In(Pr^iNCH_2)_3$], has been isolated [8].

In the present study we report some indium derivatives of the tetraaza-macrocycle, 5,7,12,14-tetramethyldibenzo [b,i] [1,6,9,10] tetraazacyclotetradecine, (H_2tmtaa) (**I**). This macrocycle was chosen since it can be considered to be intermediate between the completely aliphatic ligands (e.g. cyclam) and the aromatic porphyrin systems, and some compounds involving aluminium, and gallium alkyls have already been characterised as [Me_2Al(Htmtaa)] [11], [EtAl(tmtaa)] (**II**) [9], and [MeGa(tmtaa)] (**III**) [12]. It is of interest therefore to examine the structural variations introduced by the presence of indium, and to investigate the reactivity of In–X fragments in the macrocyclic complexes.

* Corresponding author.

[1] Dedicated to Professor Ken Wade on the occasion of his 65th birthday.

2. Results and discussion

Treatment of H_2tmtaa with an equimolar amount of $InEt_3$, in hexane at −78°C, leads to the evolution of 1 mole of ethane as the solution warms to 25°C, and the formation of [Et_2In(Htmtaa)] (**IV**) as a bright yellow precipitate which is air-sensitive. Although the product is only slightly soluble in the reaction solvent, it is highly soluble in chloroform, dichloromethane and toluene. It is noteworthy that only one of the two macrocycle N–H bonds react at 25°C, and also that no further reaction occurs even with an excess of $InEt_3$. Heating a solid sample of (**IV**) at 100°C for 1 h results in only negligible decomposition, but further heating to 145°C causes the solid to melt, and at 155°C a further mole of ethane is evolved leading to the formation of [EtIn(tmtaa)] (**V**) as a slightly air-sensitive orange solid. The same change may be effected by refluxing (**IV**) in hexane for 12 h. These transformations are similar to those observed for other Group 13 alkyl compounds in that they yield derivatives of the type (**II**) and (**III**) (see Scheme 1). The ^{1}H and ^{13}C NMR spectra are consistent with the presence of $InEt_2$ and InEt groups in (**IV**) and (**V**) respectively, and there are clear trends in the ^{13}C data as discussed below. Thermogravimetric and differential thermal analyses of (**V**), under a stream of dry nitrogen, give plots which confirm the initial melting and vapourisation (or decomposition) of (**V**) near 275°C. Although (**III**) and (**V**) are stable in chloroform, exposure of the solution to air results in demetallation of both complexes. These properties contrast with those reported for (**II**), which remains intact in wet organic solvents, whereas irradiation of a chloroform solution of (**II**) results in the formation of the monochloroaluminium compound [ClAl(tmtaa)] [9]. The lower resistance to demetallation of the Ga and In derivatives may reflect the increased distance of the metal atom from the macrocycle core. The overall reaction for the conversion (**I**) → (**IV**) → (**V**) is similar to that observed for the analogous ethylaluminium and methylgallium compounds, although (**IV**) decomposes at a lower temperature than [Me_2Ga(Htmtaa)] (225°C), but at a higher temperature than [Me_2Al(Htmtaa)] (100°C). This is consistent with both the expected higher reactivity of aluminium–carbon bonds, and the lower metal–carbon bond strength on descending the Group 13.

The X-ray crystal structure of (**V**) shows a pronounced saddle-shape of the $[tmtaa]^{2-}$ ligand with a planar array of the four nitrogen atoms [13]. The metal atom is symmetrically co-ordinated above the N_4 plane, with the axial ethyl group giving a distorted square-based pyramidal co-ordination (Figs. 1 and 2), similar to that observed in [MeIn(TPP)] [10], and the chelating amide species [MeIn{MeNC(CH)$_4$N}$_2$] and MeIn{[MeN-(CH$_2$)$_2$NMe]InMe}$_2$ [14]. In the last mentioned complex it is interesting to note that the metal atom of the MeIn fragment lies 0.93 Å above the N_4 plane, which is similar to the value observed here in (**V**). As expected, there is a sharp increase in the distance of the metal centre from the N_4 plane in (**V**) (0.91 Å), compared with the distances of 0.57 Å and 0.65 Å in (**II**) and (**III**) respectively. A consequence of the increasing size of the metal ion is that torsional distortions and angle deformations occur within the ring, so as to re-direct the nitrogen lone-pairs out of the ring, and to increase the core size of the ring. Thus the average N–Ct distance, defined as half the average distance between diagonally opposite N atoms, in (**I**), (**II**) and (**III**) of 1.90, 1.88 and 1.91 Å respectively [15], increases to 2.01 Å in (**V**). There is also a concomitant flattening of the saddle-shape in (**V**), since the average of the two dihedral angles between the N_4 plane and the planes defined by the benzenoid chelate rings (N1–N4–C17–C22) and (N2–N3–C11–C6) is only 8.4° in (**V**), but increases to

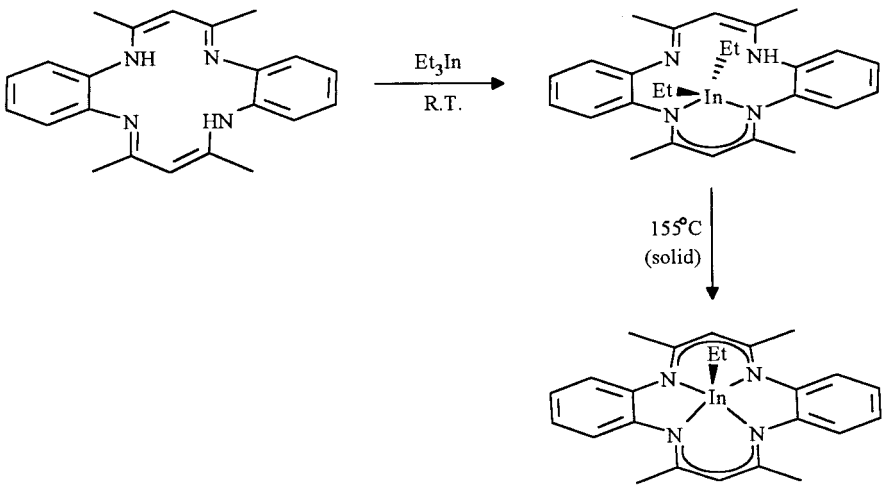

Scheme 1.

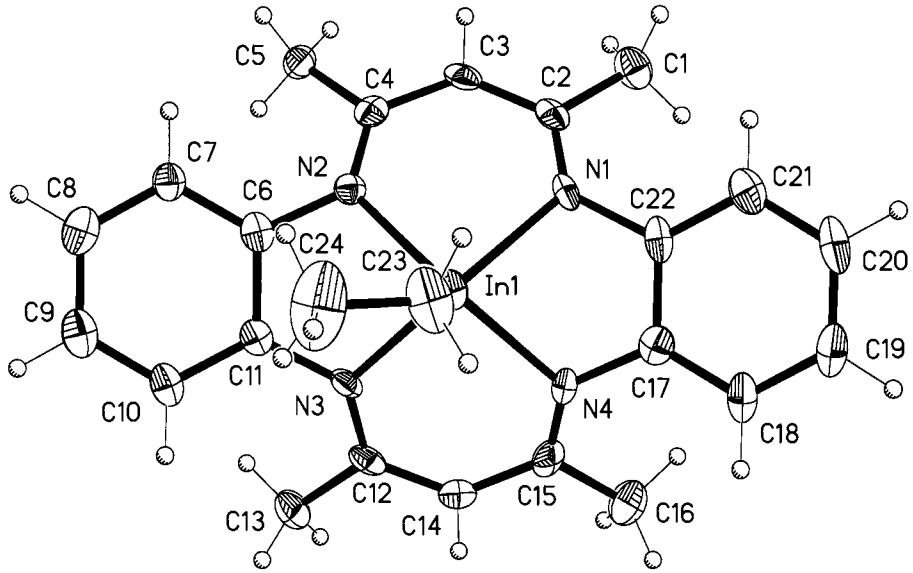

Fig. 1. The molecular structure of (**V**) showing the atom numbering.

15.9 and 14.9° in (**II**) and (**III**) respectively. The significance of these changes is illustrated by the fact that the average dihedral angle between the N_4 plane and the pentanediiminato chelate rings stays essentially constant at 33–35° in all three compounds (**II**), (**III**) and (**V**), and these values are even close to that of 35.7° observed in the free ligand (**I**) [5]. Selected bond lengths and angles for (**V**) are given in Table 1.

An alternative synthetic approach to complexes of the type [XIn(tmtaa)] involves the initial deprotonation of H_2tmtaa. The addition of a lithium alkyl ($LiMe/Et_2O$ or $LiBu^n$/hexane) to H_2tmtaa using a 2:1 molar ratio in toluene (or THF) at −78°C produces a deep red solution with gas evolution. Heating at 60°C for 2 h ensures complete reaction, and the resulting solution is extremely air and moisture sensitive changing colour rapidly to yellow on exposure to air, with reformation of the free ligand H_2tmtaa. The [Li_2(tmtaa)] salt was not isolated, but addition of the red solution to a suspension of $InCl_3$ in toluene affords [ClIn(tmtaa)] (**VI**) as an orange crystalline solid. The X-ray structure of the air-stable (**VI**) shows the familiar saddle-shaped

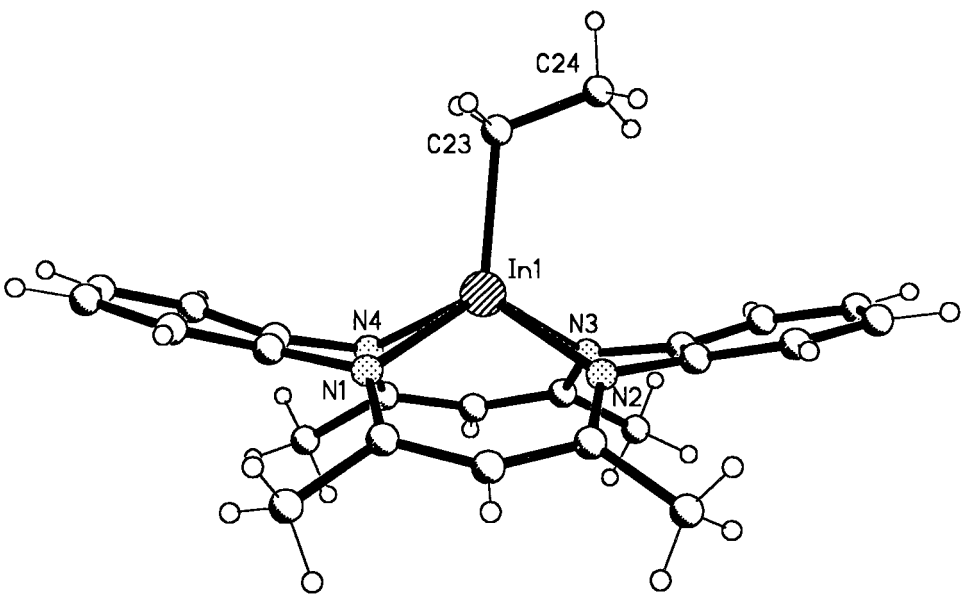

Fig. 2. The molecular structure of (**V**) showing the saddle shape of the ligand.

Table 1
Selected bond lengths [Å] and the angles [°] for (**V**)

In(1)–C(23)	2.158(6)	In(1)–N(2)	2.193(4)
In(1)–N(4)	2.207(4)	In(1)–N(1)	2.213(4)
In(1)–N(3)	2.216(4)	N(1)–C(2)	1.320(6)
N(1)–C(22)	1.431(7)	N(2)–C(4)	1.335(6)
N(2)–C(6)	1.424(7)	N(3)–C(12)	1.338(6)
N(3)–C(11)	1.403(6)	N(4)–C(15)	1.331(6)
N(4)–C(17)	1.406(7)	C(2)–C(3)	1.409(7)
C(3)–C(4)	1.400(7)	C(6)–C(11)	1.438(7)
C(12)–C(14)	1.383(8)	C(14)–C(15)	1.425(7)
C(17)–C(22)	1.430(7)		
C(23)–In(1)–N(2)	112.7(2)	C(23)–In(1)–N(4)	116.0(2)
N(2)–In(1)–N(4)	131.2(2)	C(23)–In(1)–N(1)	118.5(2)
N(2)–In(1)–N(1)	85.9(2)	N(4)–In(1)–N(4)	73.9(2)
C(23)–In(1)–N(3)	110.0(2)	N(2)–In(1)–N(3)	74.5(2)
N(4)–In(1)–N(3)	86.4(2)	N(1)–In(1)–N(3)	131.5(2)
C(2)–N(1)–C(22)	125.2(4)	C(4)–N(2)–C(6)	124.5(4)
C(12)–N(3)–C(11)	126.5(4)	C(15)–N(4)–C(17)	125.1(4)
N(1)–C(2)–C(3)	123.2(5)	C(4)–C(3)–C(2)	131.8(5)
N(2)–C(4)–C(3)	123.3(5)	N(2)–C(6)–C(11)	115.4(4)
N(3)–C(11)–C(6)	116.3(4)	N(3)–C(12)–C(14)	124.2(5)
C(12)–C(14)–C(15)	131.9(5)	N(4)–C(15)–C(14)	123.4(5)
N(4)–C(17)–C(22)	115.6(5)	C(17)–C(22)–N(1)	115.6(5)

Symmetry transformation used to generate equivalent atoms.

arrangement with the In–Cl fragment above the N_4 plane [5]. We have investigated various reactions of (**VI**) to explore the reactivity of the In–Cl bond.

Addition of LiCp (Cp = C_5H_5) to (**VI**) in toluene, using a 1:1 molar ratio, yields a deep red solution after removal of the LiCl by filtration, and dark red air-stable crystals of [CpIn(tmtaa)] (**VII**) as the solvent is removed. When (**VII**) is dissolved in dry chloroform at room temperature, significant decomposition occurs over a period of days to yield the chloro derivative (**VI**), as evidenced by the appearance of new resonances in the ^{1}H and ^{13}C NMR spectra. While such solutions can be stored at −35°C with only negligible decomposition, warming to 50–60°C causes rapid decomposition to (**VI**). The E.I. mass spectrum of (**VII**) is useful in that it shows ions at m/z values of 522 and 457, corresponding to [{CpIn(tmtaa)}$^+$] and [{In(tmtaa)}$^+$] respectively. The ^{1}H and ^{13}C NMR spectra at 25°C show only a sharp singlet for the Cp ring protons, and the carbon atoms respectively, and the spectra remained essentially unchanged at −80°C in dichloromethane solution. An X-ray structure was therefore undertaken to determine the nature of the bonding of the Cp group. The structure (Fig. 3) shows again the saddle-shape of the ligand, with the indium atom in a distorted five co-ordinate square-based pyramidal co-ordination environment. The metal is bonded to the four nitrogen atoms and to one carbon atom of the Cp group, with an In–C23 distance of 2.23 Å and the next nearest ring carbon atoms C24 and C27 being at 2.81 and 3.00 Å respectively. The metal atom is 0.83 Å above the N_4 plane, which is intermediate between the 0.74 and 0.91 Å observed for the corresponding species containing In–Cl and In–Et fragments respectively. These trends follow the expected sequence for the electron acceptor properties of these axial ligands. Selected bond distances and angles for (**VII**) are shown in Table 2.

While the η^1-bonding of the Cp ring implies the presence of two short double bonds and three longer single bonds, the observed ring bond distances and angles show a different pattern. There is one short C–C bond at 1.280(10) Å, two intermediate bonds at 1.369(10) and 1.386(10) Å, and two longer bonds at 1.449(10) and 1.439(10) Å. The internal ring angles also vary considerably from 102–113° (Fig. 4). This large variation is reflected in the non-planarity of the

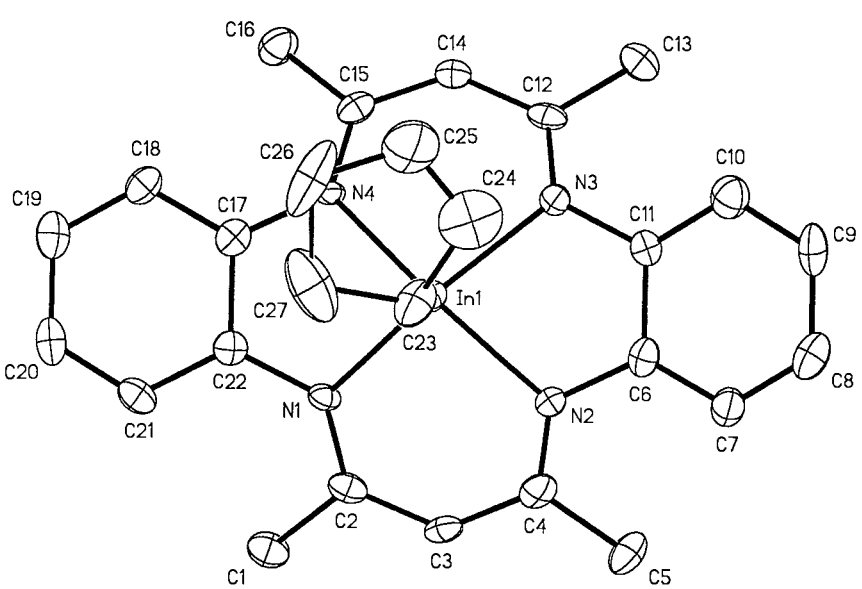

Fig. 3. The molecular structure of (**VII**) showing the atom numbering and the orientation of the Cp ring with respect to the ligand.

Table 2
Selected bond lengths [Å] and angles [°] for (**VII**)

In(1)–N(4)	2.171(4)	In(1)–N(1)	2.191(5)
In(1)–N(2)	2.191(4)	In(1)–N(3)	2.191(5)
In(1)–C(23)	2.229(6)	N(1)–C(2)	1.344(7)
N(1)–C(22)	1.412(7)	N(2)–C(4)	1.336(7)
N(2)–C(6)	1.418(7)	N(3)–C(12)	1.333(6)
N(3)–C(11)	1.426(7)	N(4)–C(15)	1.343(7)
N(4)–C(17)	1.413(7)	C(2)–C(3)	1.393(8)
C(3)–C(4)	1.408(8)	C(6)–C(11)	1.434(7)
C(17)–C(22)	1.445(7)	C(23)–C(24)	1.369(10)
C(23)–C(27)	1.439(10)	C(24)–C(25)	1.280(10)
C(25)–C(26)	1.386(10)	C(26)–C(27	1.449(10)
N(4)–In(1)–N(1)	75.7(2)	N(4)–In(1)–N(2)	136.6(2)
N(1)–In(1)–N(2)	88.5(2)	N(4)–In(1)–N(3)	88.0(2)
N(1)–In(1)–N(3)	134.4(2)	N(2)–In(1)–N(3)	74.6(2)
N(4)–In(1)–N(23)	115.4(2)	N(1)–In(1)–N(23)	111.3(2)
N(2)–In(1)–C(23)	108.0(2)	N(3)–In(1)–C(23)	114.1(2)
C(4)–N(2)–C(6)	125.9(5)	N(1)–C(2)–C(3)	124.0(5)
N(2)–C(4)–C(5)	121.0(5)	N(3)–C(11)–C(6)	115.8(5)
N(4)–C(17)–C(22)	115.7(5)		

Symmetry transformation used to generate equivalent atoms.

ring and C(23) lies 0.137(11) Å out of the plane defined as the best-fit through C(24)–C(25)–C(26)–C(27). The dihedral angle between this plane and the plane C(23)–C(24)–C(27) is 9.9(1.0)°. This value may be compared with the corresponding angles found in the monodentate rings in $In(Cp)_3$ of 2.5 and 3.2° [16]. Even though these crystallographic results do not demonstrate accurately the expected bond distances within the cyclopentadienyl ring for a η^1-bonded type, it is clear from both the ^1H and ^{13}C NMR spectra, and the thermal parameters associated with the carbon atoms of the cyclopentadienyl ring, that there is considerable rotational disorder associated with the ring. It is likely therefore that η^1-bonding does exist but that the disorder, which is not uncommon with cyclopentadienyl rings, is responsible for the deviations from a rigid η^1-model.

The reaction of (**VI**) with equimolar quantities of LiMe, $LiN(SiMe_3)_2$, and $LiOSiMe_3$ in toluene at 70°C yields [RIn(tmtaa)] [R = Me (**VIII**), $N(SiMe_3)_2$ (**IX**), $OSiMe_3$ (**X**) respectively]. These results demonstrate that the In–Cl bond is very susceptible to nucleophilic attack by the above lithium reagents. The ease with which these reactions proceed is in contrast to a recent report that Ga–Cl bond in the corresponding [ClGa(tmtaa)] does not react with LiH, $LiBEt_3H$, LiMe or [Na{$Co(CO)_4$}], although the In–Cl bond in [ClIn(tmtaa)] did react slowly with LiMe to yield [MeIn(tmtaa)] [17]. Crystals of (**VIII**), (**IX**) and (**X**), which were suitable for an X-ray study, could not be obtained, but each product is easily identified from analytical and spectroscopic data. Thus each compound shows a molecular ion in their E.I. mass spectra, and each gave a clean ^1H NMR spectrum with the appropriate integrals (see Section 3). The ^{13}C NMR data, with the assignment of the resonances, are shown in Table 3. A closer examination of these data reveals that there is a clear progression in the shift of the methine–C, the C–N carbon atoms of the pentanediiminato rings, and the aromatic C–N carbon atoms, with the predicted (and in part experimentally determined) variation of the metal–N_4 plane distance in these complexes. Using this relationship, and the similarity of the spectrum of [$(Me_3Si)_2$NIn(tmtaa)] to that of [CpIn(tmtaa)], it is suggested that both the conformation of the ligand, and the metal–N_4 distance in the solid state structure of the former, would be expected to be very similar to that observed for the latter.

In conclusion the tmtaa ligand is versatile in allowing a variety of Group 13 M–X fragments to be co-ordinated with an unusual, yet reactive, geometry around the metal atom. A range of organometallic derivatives can

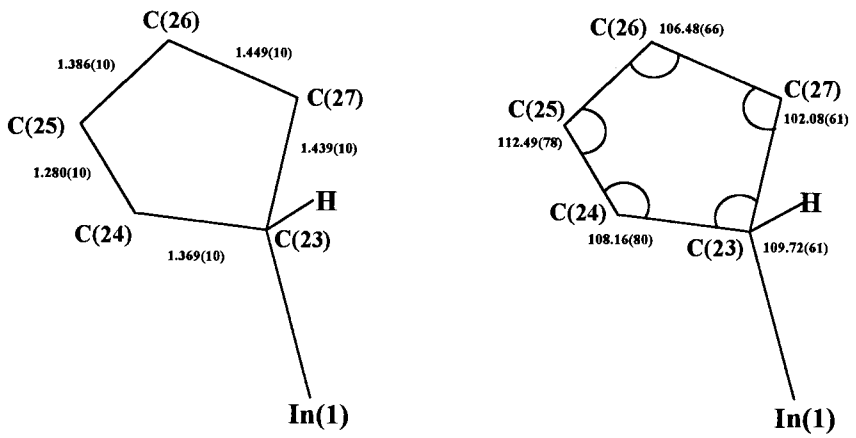

Fig. 4. The bond distances and angles within the Cp ring of (**VII**).

Table 3
Summary of proton decoupled ^{13}C NMR data (250 MHz) (δ/ppm) of [XIn(tmtaa)] compounds

Compound	Methyl–C	Methine–C	Aromatic C–H	Aromatic C–N	C–N	In axial group
[EtIn(tmtaa)]	23.38	97.02	122.84 123.80	141.80	161.39	6.67 11.22
[MeIn(tmtaa)]	23.43	97.14	122.84 123.84	141.48	161.42	[a]
[CpIn(tmtaa)]	23.87	97.55	123.20 124.00	140.61	162.13	109.84
[$(SiMe_3)_2$NIn(tmtaa)]	23.76	97.33	123.09 124.02	140.67	161.95	4.15
[$(SiMe_3)$OIn(tmtaa)]	24.23	98.51	123.25 124.14	139.84	162.95	2.51
[ClIn(tmtaa)]	24.33	98.97	123.71 124.06	139.26	163.55	–

Ran as $CDCl_3$ solution at 25°C.
[a] Not located.

be obtained, and a fuller investigation of the reactivity of such species is required to develop further the chemistry of such systems.

3. Experimental details

Air-reactive compounds were handled under argon using a conventional Schlenk or high-vacuum line, and a dry nitrogen-filled glove box. Solvents were dried and distilled under dry nitrogen prior to use. Toluene, hexane, ether and tetrahydrofuran were dried using sodium or potassium, and dichloromethane and chloroform were dried over calcium hydride. NMR solvents were dried over 4 Å molecular sieves before use.

The ^1H and ^{13}C NMR spectra were recorded using either a Bruker Associates ACF250 or ACP400 spectrometer, with chemical shifts quoted relative to TMS and with negative shifts being to high field. Elemental analyses were carried out using a Leco CHNS 932 or a Perkin Elmer 2400 elemental analyser. Thermal analyses were carried out using a Stanton STA 1000 instrument, and mass spectra were recorded using a Kratos MS80 spectrometer, or data were obtained from the EPSRC mass spectrometry service at the University of Swansea.

The ligand H_2tmtaa was synthesised by the literature method [18]; all other chemicals were obtained from commercial suppliers, and used without further purification.

3.1. Preparation of [Et_2In(Htmtaa)] (IV)

A solution of $InEt_3$ (0.39 g, 1.93 mmol) in hexane (20 cm^3) was added to a suspension of H_2tmtaa (0.63 g, 1.83 mmol) in hexane at −78°C. Evolution of ethane occurred as the solution was warmed to 25°C over 1 h. A yellow solid slowly deposited, and after cooling and filtering the solid was pumped in vacuo for 2 h to give a lemon yellow powder. Yield 0.8 g (85%). Anal. Calc. for $C_{26}H_{33}N_4In$: C, 60.5; H, 6.4; N, 10.8. Found: C, 60.8; H, 6.3; N,10.7%. ^1H NMR (400 MHz)($CDCl_3$), δ/ppm, −0.02, 0.72 (2 × q, 2 × 2H, InCH_2CH_3); 0.47, 1.38 (2 × t, 2 × 3H, InCH_2CH_3); 1.65, 2.11 (2 × s, 2 × 6H, CH3); 4.82, 4.84 (2 × s, 2 × ^{1}H, methine CH); 6.97–7.10 (m, 8H, C_6H_4); 12.24 (s, ^{1}H, NH).

3.2. Preparation of [EtIn(tmtaa)] (V)

The diethylindium complex [Et_2In(Htmtaa)] (0.40 g, 0.78 mmol) was refluxed in hexane for 12 h. Deep orange crystals were deposited on cooling. Yield 0.24 g (64%). This procedure is convenient for obtaining good quality crystals of (**V**), but an essentially quantitative conversion of (**IV**) to (**V**) can be achieved by heating a solid sample of (**IV**) to 180°C under dry nitrogen. Anal. Calc. for $C_{24}H_{27}N_4In$: C, 59.3; H, 5.6; N, 11.5. Found: C, 59.4; H, 5.4; N, 11.5%. ^1H NMR (400 MHz), ($CDCl_3$), δ/ppm, 0.34 (q, 2H, InCH_2CH_3), 0.76 (t, 3H, In$CH_2\mathbf{CH_3}$), 4.66 (s, 2H, methine CH), 6.90–7.10 (AA′BB′ multiplet, 8H, C_6H_4). The mass spectrum (E.I.) gave a molecular ion at $m/z = 486$, and other ions at 457[$(M–Et)^+$] and 344[$(M–Et–In)^+$].

3.3. Preparation of [ClIn(tmtaa)] (VI)

Lithium methyl (10.4 cm^3, 14.5 mmol) in ether was added to a solution of H_2tmtaa (2.5 g, 7.3 mmol) in toluene (70 cm^3) at −78°C. The mixture was then warmed to 60°C for 2 h, and the resulting red solution was transferred through a cannula into a suspension of $InCl_3$(1.6 g, 7.3 mmol) in toluene at −78°C. After heating at 70°C for 2 h, and cooling and filtering, a dark orange solution was obtained. After reducing the filtrate to 20 cm^3, addition of hexane precipitated a dark orange solid, which was collected by filtration and dried by

pumping in vacuo for 2 h. Yield 2.4 g (68%). Anal. Calc. for $C_{22}H_{22}N_4ClIn$: C, 53.6; H, 4.5; N, 11.4. Found: C, 54.0; H, 4.4; N, 11.3%. ^{1}H NMR (250 MHz), ($CDCl_3$), δ/ppm, 2.27 (s, 12H, CH_3), 4.80 (s, 2H, methine CH), 6.98–7.18 (AA′BB′ multiplet, 8H, C_6H_4). The mass spectrum shows ions at $m/z = 492(M^+$ based on ^{35}Cl), 327[(M–In–Cl–Me)$^+$] and ions from tmtaa at e.g. 132[$(C_6H_4NC_3)^+$] and 65[$(NCCH_3C2)^+$].

3.4. Preparation of [MeIn(tmtaa)] (VIII)

An ethereal solution of LiMe (0.9 cm^3, 1.3 mmol) was added to a stirred solution of [ClIn(tmtaa)] (0.65 g, 1.3 mmol) in toluene at −78°C. After warming to 70°C for 3 h, cooling and filtration gave a deep orange filtrate which deposited orange crystals after concentration. Yield 0.4 g (66%). Anal. Calc. for $C_{23}H_{25}N_4In$: C, 58.5; H, 5.3; N, 11.9. Found: C, 58.9; H, 5.4; 11.6%. ^{1}H NMR (250 MHz), ($CDCl_3$), δ/ppm, −0.63 (s, 3H, $InCH_3$), 2.15 (s, 12H, CH_3), 4.65 (s, 2H, methine CH), 6.92–7.07 (AA′BB′ multiplet, 8H, C_6H_4). Mass spectrum gave ions at $m/z = 472(M^+)$, 457[(M–Me)$^+$], 327[(M–In–Me–Me)$^+$].

3.5. Preparation of [XIn(tmtaa)] [X = Cp, $(Me_3Si)_2N$, $(Me_3Si)O$]

The above complexes were prepared using a similar procedure to that used for [MeIn(tmtaa)]. A summary of the experimental details is given below.

3.5.1. Preparation of [CpIn(tmtaa)] (VII)

Reagents: [ClIn(tmtaa)] (1.8 g, 3.7 mmol), LiCp (0.3 g, 3.7 mmol). Product is a brick-red solid. Yield 1.2 g (60%). Anal. Calc. for $C_{27}H_{27}N_4$ In: C, 62.1; H, 5.2; N, 10.7. Found: C, 63.2; H, 5.3; N, 10.2%. ^{1}H NMR (400 MHz), ($C_6D_5CD_3$), δ/ppm, 1.87 (s, 12H, CH_3), 4.42 (s, 2H, methine CH), 6.03 (s, 5H, C_5H_5), 6.89 (s, 8H, C_6H_4). The mass spectrum gave ions at $m/z =$ 522(M^+), 457[(M–C_5H_5)$^+$], 132[$(C_6H_4NC_3)^+$]. Crystals suitable for X-ray analysis were grown from toluene solution.

3.5.2. Preparation of $[(Me_3Si)_2NIn(tmtaa)]$ (IX)

Reagents: [ClIn(tmtaa)] (1.1 g, 2.2 mmol), [$LiN(SiMe)_2$] (0.6 g, 2.2 mmol). Product recrystallised from toluene as a yellow/orange solid. Yield 0.85 g (63%). Anal. Calc. for $C_{28}H_{40}N_5InSi_2$: C, 54.4; H, 6.5; N, 11.3. Found: C, 54.4; H, 6.6; N, 11.0%. ^{1}H NMR (250 MHz), ($CDCl_3$), δ/ppm, −0.24 [s, 18H, $(SiMe_3)_2$], 2.20 (s, 12H, CH_3), 4.76 (s, 2H, methine CH), 6.95–7.15 (AA′BB′ multiplet, 8 H, C_6H_4). The mass spectrum gave ions at $m/z = 617(M^+)$, 457[(M–$N(SiMe_3)_2$)$^+$], 132[$(C_6H_4NC_3)^+$].

3.5.3. Preparation of $[(Me_3Si)OIn(tmtaa)]$ (X)

Reagents [ClIn(tmtaa)] (0.8 g, 1.7 mmol), [$LiOSiMe_3$] (0.2 g, 1.7 mmol). The product was recrystallised from toluene as an orange solid. Yield 0.6 g (60%). Anal. Calc. for $C_{25}H_{31}N_5InOSi$: C, 53.6; H, 5.6; N, 12.5. Found: C, 54.2; H, 5.5; N, 12.4%. ^{1}H NMR (250 MHz), ($CDCl_3$), δ/ppm, −0.34 (s, 9 H, $SiMe_3$), 2.25 (s, 12 H, CH_3), 4.75 (s, methine CH), 6.94–7.17 (AA′BB′ multiplet, 8H, C_6H_4). The mass spectrum gave ions at $m/z = 546(M^+)$, 457[(M–$OSiMe_3$)$^+$], 132[$(C_6H_4NC_3)^+$].

3.6. X-ray crystallography

For both compounds (**V**) and (**VII**) accurate cell parameters (from 250 reflections) and intensity data were collected using a Delft Instrument with a FAST TV area detector, and with MoK X-rays ($\lambda = 0.71073$ Å) [19]. Data collection: MADNES [20]; cell refinement: MADNES; data reduction: SHELXTL-Plus [21]; program(s) used to solve structures: SHELXTL-Plus; programs used to refine structures: SHELXTL 93 [22]; molecular graphics: SHELXTL-Plus; software used to prepare material for publication: SHELXTL 93. The data collected for both compounds were corrected for Lorentz and polarisation effects. All non-hydrogen atom positions were located by direct methods. Hydrogen atoms were added at calculated positions and given fixed isotropic thermal parameters. Anisotropic displacement parameters were refined for all non-hydrogen atoms.

Deep orange, rectangular block crystals of (**V**) were obtained by recrystallisation from hot hexane solution. A crystal of dimensions $0.24 \times 0.20 \times 0.18$ mm was chosen for X-ray diffraction analysis, and mounted under argon in a thin walled quartz Lindemann tube. A total of 9346 reflections in the range $1.97 < \theta 25.08°$ were collected at 140(2)K, of which 3269 were unique.

3.6.1. Crystal data: $C_{24}H_{27}N_4In$

$M_r = 486.32$, monoclinic, space group $P2_1/n$. Unit cell dimensions: $a = 10.014(2)$, $b = 16.092(3)$, $c =$ 13.507(3) Å, $\beta = 94.98(3)°$, $U = 2168.4(8)$ Å^3, $D_c =$ 1.4909 g cm^{-3}, $Z = 4$, $F(000) = 992$, $\mu = 1.107$ mm^{-1}.

The refinement converged with $R1$ ($I/\sigma(I) > 2.0$) $= 0.0395$ for 2278 data, 0.0620 for all data: $wR2 =$ 0.0878 ($I/\sigma(I) > 2.0$), 0.0923 for all data, and GoF on $F^2 = 0.872$. The final difference map showed no peaks or holes of electron density greater than +1.102 e Å^{-3} and −0.438 e Å^{-3}.

Brick-red, well defined rectangular blocks of (**VII**) were obtained by controlled cooling of a saturated hot toluene solution. A crystal of dimensions $0.28 \times 0.16 \times$ 0.18 mm was chosen for the X-ray analysis. A total of

9430 reflections in the range $1.97 < \theta 25.08°$ were collected at 150(2)K, of which 3372 were unique.

3.6.2. Crystal data: $C_{27}H_{27}N_4In$

$M_r = 522.04$, monoclinic, space group $P2_1/n$. Unit cell dimensions $a = 10.283(7)$, $b = 15.545(7)$, $c = 13.864(2)$ Å, $\beta = 92.04(9)°$, $U = 2215(2)$ Å^3, $D_c = 1.567$ g cm^{-3}, $Z = 4$, $F(000) = 1064$, $\mu = 1.090$ mm^{-1}.

The refinement converged with $R1$ $[I/\sigma(I) > 2.0] = 0.0406$ for 2453 data, 0.0576 for all data: $wR2 = 0.0970$ $[I/\sigma(I) > 2.0]$, 0.1017 for all data, and GoF on $F^2 = 0.949$. The final difference map showed no peaks or holes of electron density greater than $+1.334$ e Å^{-3} and -0.454 e Å^{-3}.

Complete bond lengths and angles, final positional parameters, thermal parameters and calculated hydrogen atom positions for compounds (**V**) and (**VII**) have been deposited at the Cambridge Crystallographic Data Centre.

Acknowledgements

We thank the EPSRC and the Associated Octel Co. Ltd. for grants in support of this work. We also thank the EPSRC X-ray service at the University of Cardiff, and the mass spectrometry service centre at University of Swansea for data collection.

References

[1] N.F. Curtis, Comp. Coord. Chemistry., Vol. 2, R.D. Gillard, J.A. McCleverty, G. Wilkinson (Eds.), Pergamon, 1987, p. 899.
[2] R. Guilard, K.M. Kadish, Chem. Rev. 88 (1988) 1121.
[3] T. Aida, S. Inoue, Acc. Chem. Res. 29 (1996) 39.
[4] D. Takeuchi, Y. Watanabe, T. Aida, S. Inoue, Macromolecules 28 (1995) 651.
[5] P.R. Phillips, A. McCamley, N.W. Alcock, M.G.H. Wallbridge, Acta Cryst. C50 (1994) 1072.
[6] M.J. Taylor, D.G. Tuck, L. Victoriano, J. Chem. Soc., Dalton Trans. (1981) 928.
[7] A. Tabard, R. Guilard, K.M. Kadish, Inorg. Chem. 25 (1986) 4277.
[8] D.C. Bradley, D.M. Frigo, I.S. Harding, M.B. Hursthouse, J. Chem. Soc., Chem. Commun. (1992) 577.
[9] V.L. Goedken, H. Ito, J. Chem. Soc., Chem. Commun. (1984) 1453.
[10] C. Lecomte, J. Protas, P. Cocolios, R. Guilard, Acta Cryst. B36 (1980) 2769.
[11] J.C. Cannadine, W. Errington, P. Moore, M.G.H. Wallbridge, E. Nield, D. Fenn, J. Organomet. Chem. 486 (1995) 237.
[12] N.W. Alcock, N.C. Blacker, W. Errington, M.G.H. Wallbridge, Acta Cryst. C49 (1993) 1359.
[13] F.A. Cotton, J. Czuchajowska, Polyhedron 9 (1990) 2553.
[14] A.M. Arif, D.C. Bradley, H. Dawaes, D.M. Frigo, M.B. Hursthouse, B. Hussain, J. Chem. Soc., Dalton Trans. (1987) 2159.
[15] V.L. Goedken, J.J. Pluth, S.M. Peng, B. Bursten, J. Am. Chem. Soc. 98 (1976) 8014.
[16] F.W.B. Einstein, M.M. Gilbert, D.G. Tuck, Inorg. Chem. 11 (1972) 2832.
[17] D.A. Atwood, V.O. Atwood, A.H. Cowley, Inorg. Chem. 31 (1992) 3871.
[18] V.L. Goedken, M.C. Weiss, Inorg. Synth. 20 (1980) 115.
[19] J.A. Dow, S.R. Drake, M.B. Hursthouse, K.M. Malik, Inorg. Chem. 32 (1993) 5704.
[20] J.W. Pflugrath, M. Messerschmidt, Munich Area Detector Systems, Enraf-Nonius, Delft, Netherlands.
[21] G.M. Sheldrick, SHELXTL-Plus, Release 4.1, Siemens Analytical X-ray Instruments, Madison, Wisconsin, USA, 1991.
[22] G.M. Sheldrick, SHELXTL 93, Program for the Refinement of Crystal Structures, University of Göttingen, Germany, 1993.